6. Low Power Radar front-end for e-health and harbour surveillance: implementation examples

6.1 Summary

In this chapter two case studies of low-power/low-cost RADAR front-end for specific applications are presented, starting from the problem description up to the design, simulation and realization of the prototypes. The emphasis is on the radio front-end circuits whose design and simulation has become much easier than in the past thanks to modern simulation tools and accurate high frequency device modeling. At the same time, the unitary cost of new generation integrated RADAR sensor has reduced by orders of magnitude thanks to the utilization of modern Integrated Circuit technologies. The front-end contains all of the radiofrequency circuits and subsystems necessary to generate the waveform to be transmitted, together with the output and input RF filters, low noise amplifier, mixer and so on. The output of the RADAR receiver can be AD converted and digital elaboration can be accomplished by purposely designed integrated Digital Signal Processor or by traditional elaboration tools running on an external elaboration system, typically a PC. Although the emphasis is mainly on circuits and subsystems, some basic information will be given about the antennas and the digital signal processing used to test the prototypes.

The first case we present is a miniaturized pulsed E-Health (EH) RADAR for non invasive continuous monitoring of heart and breath activities, which does not require digital elaboration. The second one is a low power RADAR front-end for Harbour Surveillance (HS). In this second case the output of the radio front-end receiver is sampled and elaborated by an external system even if, in the future, a dedicated DSP could be embedded in a multi chip module together with the radio interface for more compact, cheaper and less power consuming solution.

For the design and realization of EH RADAR an entirely integrated solution was chosen in that it was possible to foresee a large scale production of the device, whose main utilization could be the monitoring of cardiopatic patients during the normal activities of their life or the monitoring of the breathing activity of sleeping adults or infants affected by recurrent apneas. It is well known that, for large and very large production scale the more suited solution consist of a fully integrated system on a single chip: the feasibility study and design are presented in this chapter, whereas related technologies have been described and discussed in Chapter 2.

For the design and realization of HS RADAR, instead, a small scale production has been foreseen: some tens of devices for each harbour, thousands of pieces in total. For this reason a hybrid solution was chosen, that is discrete devices mounted on a substrate in which passive devices (matching networks, filters, power divider and combiners an so on) are integrated. This solution does not require the utilization of sophisticated technological processes and, consequently, the access to a silicon foundry. It can be realized in any electronic laboratory equipped with a photo-lithographic etching process and a work station for bonding. Hybrid circuits for RF and Microwave applications, commonly called Microwave Integrated Circuits (MIC), represent the best solution for small and medium scale production and for prototype realization. Section 6.3 of this chapter is entirely dedicated to a concise description of the hybrid technology for MIC design and realization.

6.2 Miniaturized RADAR for E-Health

A portable RADAR system can allow the monitoring in a contactless way of some vital functions such as the heart activity and the respiratory one. In fact, the movement of the heart walls, as well as the slower one of the chest due to the breath, interact with the transmitted electromagnetic wave and modulate the back scattered one. Both Continuous Wave (CW) RADAR, using the Doppler effect, and pulsed RADAR, measuring the change of distance between the radar sensor and the target, can be used. In the case of the respiratory activity, which is characterized by slow movements in a frequency range about five times lower than cardiac frequency, the pulsed RADAR is more effective. In fact the shift Doppler Δf depends on the target velocity V_R, on the frequency f_0 and on the propagation velocity c of the transmitted wave through the relationship:

$$\Delta f = 2\frac{v_R}{c} f_0 \qquad (6.1)$$

Eq. 6.1, for f_0 = 10 GHz, an estimated chest velocity v_R of a few centimeter per second, gives a value of Δf in the range of a few Hertz (for c the value of the EM wave phase velocity in vacuum/air has been used). An output signal in this frequency range is very difficult to be monitored mainly due to: i) the low frequency fluctuations of the amplifier offset; ii) the flicker noise affecting the operations of any electronic devices at low frequencies. These causes of disturbances cannot be eliminated by using a low pass filter in that they are located in the same frequency range of the signal. For this reason a pulsed RADAR solution has been preferred.

In the past, several realizations have been presented of single chip (or chipset) implementing the RADAR for biomedical applications [1-8]: we will refer here to that described in [6] and [7].
The block scheme of the system is described in Fig. 1 in which an Ultra Wide Band (UWB) pulsed RADAR solution is presented [6-7].

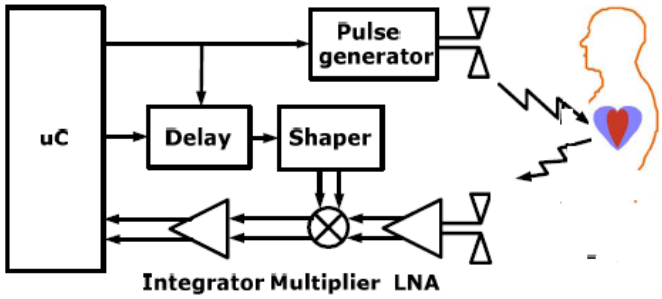

Fig. 1 Block diagram of a pulsed RADAR for biomedical applications [7].

The term UWB applies in case the frequency band occupied by the signal is at least 500 MHz or more than 20% of the central frequency. To this kind of application (UWB modulation) a frequency range starting from 3.1 up to 10.6 GHz has been dedicated by international organizations (FCC for USA, ETSI for Europe etc.). This frequency range can be utilized without any authorization (unlicensed band) provided that the Effective Isotropic Radiated Power Spectral Density of the transmitted signal is lower than -41.3 dBm/MHz.
The transmitted pulse is partially reflected at each interface it passes through: air / skin, muscle / bone, bone / addominal cavity, addominal cavity / heart wall and so on. In this way an echo is generated at each interface: for each transmitted pulse several echoes with different delays are back scattered to the receiving antenna. By choosing a suited value of the delay introduced by the delay block in Fig. 1, the replica of the transmitted pulse generated by the shaper arrives at the multiplier input together with the echo coming from the selected interface. The output of the multiplier is different from zero just during the time interval in which delayed and reflected pulses superimposed at the multiplier input. So that, the output of the Integrator (a low pass filter) attains its maximum when the pulses perfectly coincide, whereas it goes to zero when they do not superimpose at all. The small cyclic movement of the interface causes a cyclic variation of the reciprocal delay between the replica of the pulse generated by the shaper and the echo received by the receiving antenna, so causing a cyclic variation of the output of the integrator. For a continuous monitoring of the instantaneous displacement $\Delta x(t)$ of the interface from a reference position, the pulse duration

ΔT should be equal to twice the time the EM wave takes to cover a distance equal to the maximum (Δx_{MAX}) of Δx: that is $\Delta T = 2\,\Delta x_{MAX}/c$. In fact, if the delay time is set in such a way that, when Δx=0, delayed and reflected pulses completely superimpose each other at the multiplier input, then, when $\Delta x = \Delta x_{MAX,}$ their reciprocal delay at the multiplier input will be ΔT, and the time interval in which they superimpose will be nulled. However, ΔT values larger than $2\Delta x_{MAX}/c$ can be used, provided that a reduction of the dynamic of the signal at the output of the integrator can be tolerated. In fact, in this case a partial superimposition between reflected and delayed pulses is present even when $\Delta x = \Delta x_{MAX}$. For instance, if $\Delta T = 4\Delta x_{MAX}/c$, when Δx=0 the two pulses are completely coincident at the multiplier input, whereas when $\Delta x = \Delta x_{MAX}$ they are superimposed for a time equal to $2\Delta x_{MAX}/c$ that is $\Delta T/2$. In this case the output of the integrator will change between V_{MAX} (Δx=0) and V_{MAX} /2 ($\Delta x = \Delta x_{MAX}$) instead of between V_{MAX} and zero. This discussion shows that values of the pulse duration slightly larger than "*twice the time the EM wave takes to cover a distance equal to the maximum (Δx_{MAX}) of Δx* " can be used without a drastic lack of sensitivity of the RADAR sensor. With reference to the breath monitoring we can suppose Δx_{MAX} = 3 cm at which a value of $\Delta T = 2\,\Delta x_{MAX}/c$ = 200 ps would correspond. For the calculus, the light velocity in air has been used for c: this fact implies that the interface to be monitored moves in air (breath monitoring), otherwise the proper phase velocity in the medium should be used. In [9] the relative permittivity of some biological tissues are reported: the typical values at 10 GHz are around 10, corresponding to a propagation velocity three times (or more) slower than in air. A value of ΔT slightly higher is obtained in the case of heart monitoring, in fact the cardiac walls displacement is around 1.5 cm, but the propagation velocity is reduced by about 1/3. In the prototype of the EH RADAR which has been realized and tested, variable ΔT between 200 and 400 ps has been chosen, in order to relax the specifications on the Pulse Generator (PG) design.

A preliminary feasibility study has demonstrated the possibility of realizing the entire transmitter/receiver section in a single chip.

By supposing a power supply voltage of 1.2 V, a differential output voltage of 900 mV at the transmitter output, a differential signal of 650 mV at the transmitting antenna input (a voltage drop of 0.25 V due to the cables has been considered) and a differential antenna impedance of 100 Ω, then the transmitted power during the pulse, supposed sinusoidal shaped, is 0.528 mW. In order to estimate the available power at the input of the receiving antenna, the attenuation between transmitted and received pulse must be calculated. A rough estimation, confirmed also by other similar cases presented in literature [6 and 7 references therein], indicates, for heart monitoring, a value of the attenuation of about 80 dB due to path loss, to the reflection coefficient smaller than 1

at the interfaces, and to the attenuation inside the biological tissues. It must be noted that, in the case of heart monitoring, the transmitting antenna is put in contact with the chest, so that far field equations for propagation and attenuation of EM wave cannot be used and near field equations have to be used. Details about this modelization are given in [6]. The attenuation is much smaller in the case of breath monitoring in that the antennas are put a few tens of centimetres from the chest and the interface to be monitored is that between air and skin, so that no attenuation inside the biological tissues has to be considered. In the worst case (80 dB attenuation), a value of the reflected available power at the receiving antenna input $P_{AIN}=5.28\text{x}10^{-12}$ W can be hypothesized. This value corresponds, at T_0=290K, to a Signal to Noise Ratio (SNR_{OUT}) at the output of the LNA, for a single pulse, given by the following relationship:

$$SNR_{OUT} = \frac{P_{AIN}}{kT_0BN_F} \qquad (6.2)$$

where N_F is the LNA Noise Figure, B=7.5 GHz (from 3.1 to 10.5 GHz) is the LNA band for UWB signal, k the Boltzmann constant. The denominator of (2) should be substituted by $kB\left[T_0\left(N_F-1\right)+T_i\right]$ if the absolute temperature at which the input of the amplifier is terminated was T_i. By using a prudential value of 10 dB for N_F, T_i = 298 K (25°C) (breath monitoring), Eq. 6.2 gives a value of SNR_{OUT} of about -18 dB. The situation would appear just a bit worse for heart monitoring: in this case Ti=37°C which is the mean temperature of human body. This value of SNR_{OUT} could appear too small for a correct detection of the back scattered pulse at the receiver output. At this point, it must be considered that the pulse are repeated with a pulse rate P_R between 1 and 40 MHz, and that the output of the multiplier can be integrated for a given time T_{INT}. The choice of the integration time T_{INT} must be done by taking into account two different limitations. In fact, T_{INT} has to be quite long to maximize the signal to noise ratio without infringe upon the conditions for time resolution required for monitoring the phenomenon under observation. The period of the phenomena under observation is between 0.5 s (heart) and 10 s (breath). So that, an integration time of about 1/100 of the period of the fastest phenomenon under observation can be considered suited for a continuous monitoring with a sufficient time resolution. By using T_{INT}=5ms (both the heart and the chest displacement can be considered negligible in 5 ms) and P_R=2 MHz, 10.000 quite identical and fully correlated pulses occur in T_{INT}. By integrating the output of the multiplier with a time constant equal to T_{INT} an improvement of 40 dB (10Log10,000) of SNR_{OUT} is obtained. Consequently, the resultant value of SNR_{OUT} rises up from -18 to +22 dB, which can be

considered well suited for a detailed analysis of the phenomenon under observation. This quite rough estimation demonstrates, at a first approach, the possibility to realize in a fully integrated way the RADAR sensor. In fact, the pulse duration (200-400 ps), the output power (0.528 mW with a power supply voltage of 1.2 V), the receiver Noise Figure (less than 10 dB) can be obtained by using a well consolidated technology among those which are available on the market. The fully integrated RADAR sensor has been designed, simulated and realized by using the 90 nm CMOS technology by STMicroelectronics. After the chip realization, the single blocks of the prototype have been characterized by means of a purposely designed test bench.

The schematics of the building blocks of the front end [7] are shown in Fig. 2. A differential topology has been chosen starting from pulse generator output up to antennas and, in receiving section, for LNA, multiplier and integrator. A square wave generator with a maximum frequency P_R= 10 MHz is integrated in order to generate a triangular wave which, in turn, is shaped by a shaping network (SN in Fig.2) whose output is a bipolar Gaussian like pulse. This shape of the pulse has been chosen to comply with the regulation requirement for UWB communication in term of power spectral density mask. The output of the shaper is connected by a short differential cable to the transmitting antenna.

The receiving antenna, with the same characteristics of the transmitting one, receives the back scattered echoes which are pulses similar to the transmitted ones, even if a given level of linear distortions has to be taken into account due to the effect of the crossing of biological tissues and the reflection at the interfaces. The antenna gain used for testing was a slotted antenna with a gain of 10 dB realized on a soft substrate [10], whereas a purposely designed antenna, for use in respiratory activity monitoring, realized in FR4 has been described in [11].

The LNA topology is a three stages: common gate followed by two common source differential stages. The main characteristics of LNA are: Gain = 22.7 dB @ 5 GHz, return loss S_{11}<-10.5 dB, NF = 6.5 dB, 1dB compression point $1dB_{CP}$= -19.7 dBm, dissipated power P_D= 34.8 mW. A P-MOS Gilbert cell implements the multiplier, whose power consumption is 3.7 mW. The multiplier output is sent to the differential integrator which is implemented by means of a simple RC low pass filter preceded and followed by two stages which introduce a total voltage gain of 58 dB.

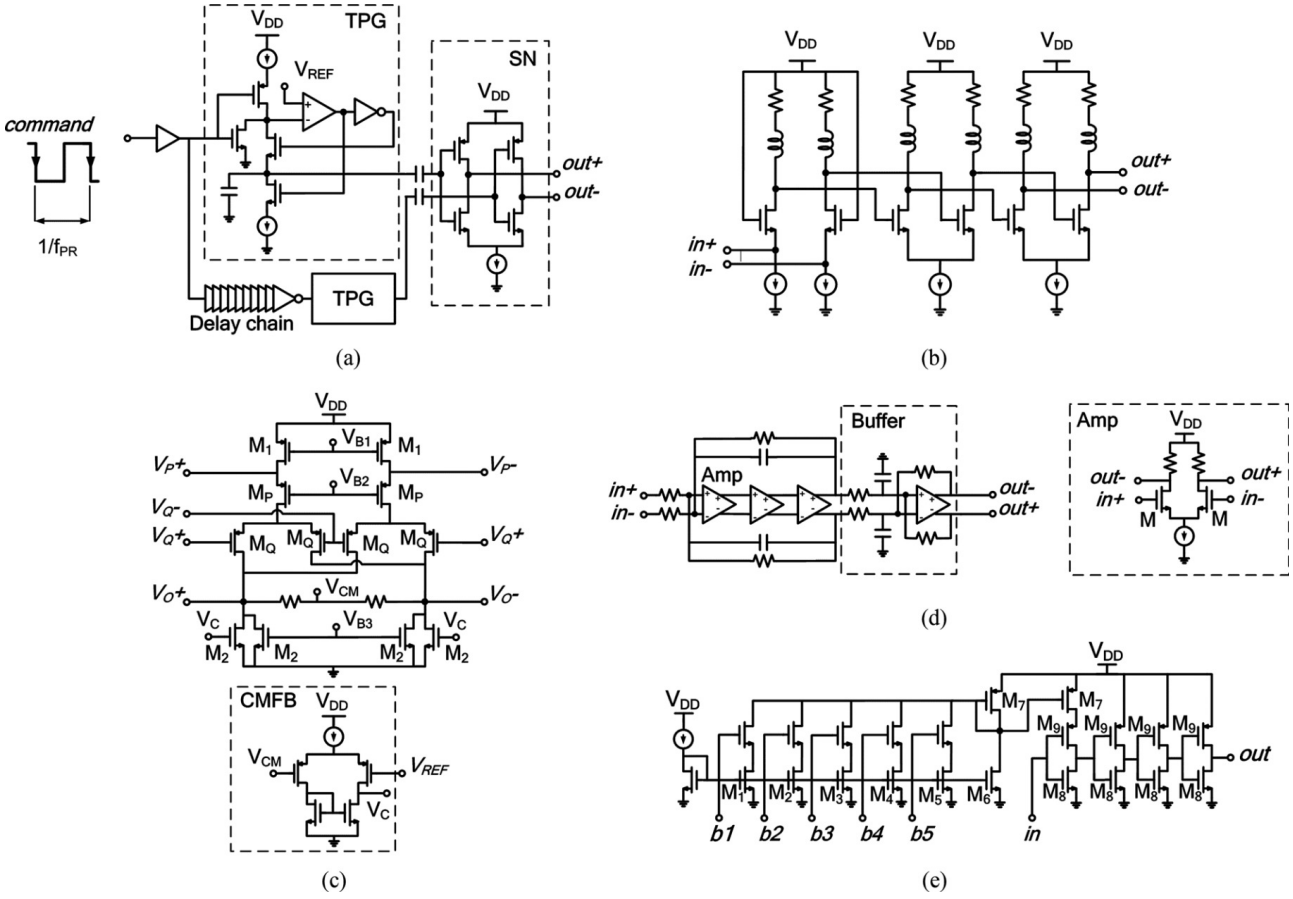

Fig. 2 Schematic of the building blocks of EH RADAR front-end [7]: (a) Pulse generator, (b) LNA, (c) Multiplier, (d) Integrator, (e) Delay Generator; V_{DD}=1.2V.

In Fig. 3 the micrograph of the RADAR test chip is shown: the occupied area on silicon die is 1.5x1.3 mm^2. For testing, the die has been mounted on a QFN32 package for testing whose external dimensions are 5x5 mm^2, whereas the antennas, whose dimensions are in the range of some centimeters, depending on the required gain, could be realized in the future on a polymeric flexible substrate and "embedded", together with the RADAR microchip in a T-shirt realizing the first prototype of a "wearable RADAR". The characteristic of the integrated EH RADAR front-end, together with the small value of the total power consumption, only 73.2 mW, makes the EH RADAR well suited to be "weared" by cardiopatic patients which could be equipped with an RF interface (for instance Bluetooth or Zigbee) for data transmission to a base station or to a storage device for a continuous, not invasive monitoring during their normal activities.

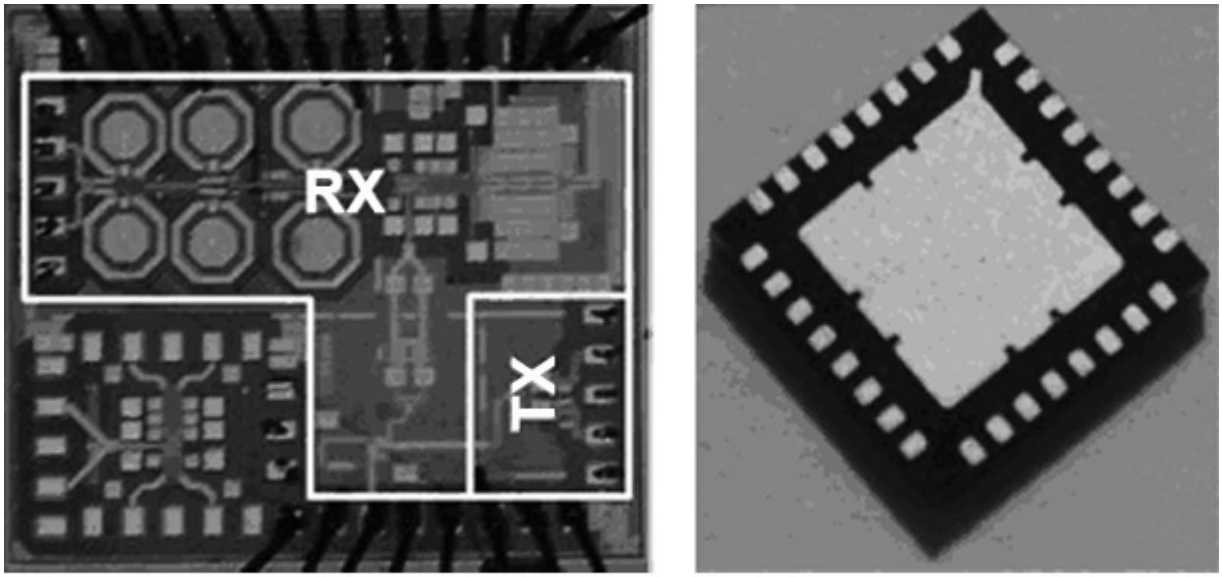

Fig. 3 Micrograph of the EH RADAR front-end chip (a) and of the QFN32 in which it has been mounted (b) [7]. The die size is 1.5x1.3 mm^2.

A prototype of EH RADAR front-end has been successfully tested for the contactless monitoring of the breathing activity in patients affected by nocturnal apneas and for the monitoring of babies during their sleep in order to prevent the phenomenon of crib deaths [7].

6.3 Microwave Integrated Circuit

The term Microwave Integrated Circuits (MIC) refers to RF and Microwave circuits realized by integrating both passive and active devices in the same planar substrate. More in details, for passive devices (resistances, capacitors, inductors), two possibilities are available: i) they can be realized directly on the substrate; ii) they can be purchased in packaged or in chip version and bonded on the substrate. For active devices, just the second possibility is available since it is not possible to realize them directly on the substrate. For this reason, it would be more appropriate to use the term "Hybrid Circuits" for MIC, since this technology makes use of devices directly realized on the substrate together with discrete devices previously realized elsewhere then bonded on the substrate.

MIC are composed of: i) the substrate, ii) the passive devices, iii) the active devices. To these three components it must be added the connectors and the case which are essential to realize the link with other blocks of the system and to give a suitable shielding effect. The latter functionality is very

important in order to avoid cross talk between different blocks, to reduce the effect of interferences and external noise, to guarantee the stability of the active stages.

In Fig. 4 a typical MIC realization is shown: the upper case has been removed to show the planar substrate with active and passive devices. In the figure some typical distributed passive devices realized with a photo-lithographic process are also shown. A detailed analysis of theory and application of planar technology can be found, for instance, in [12].

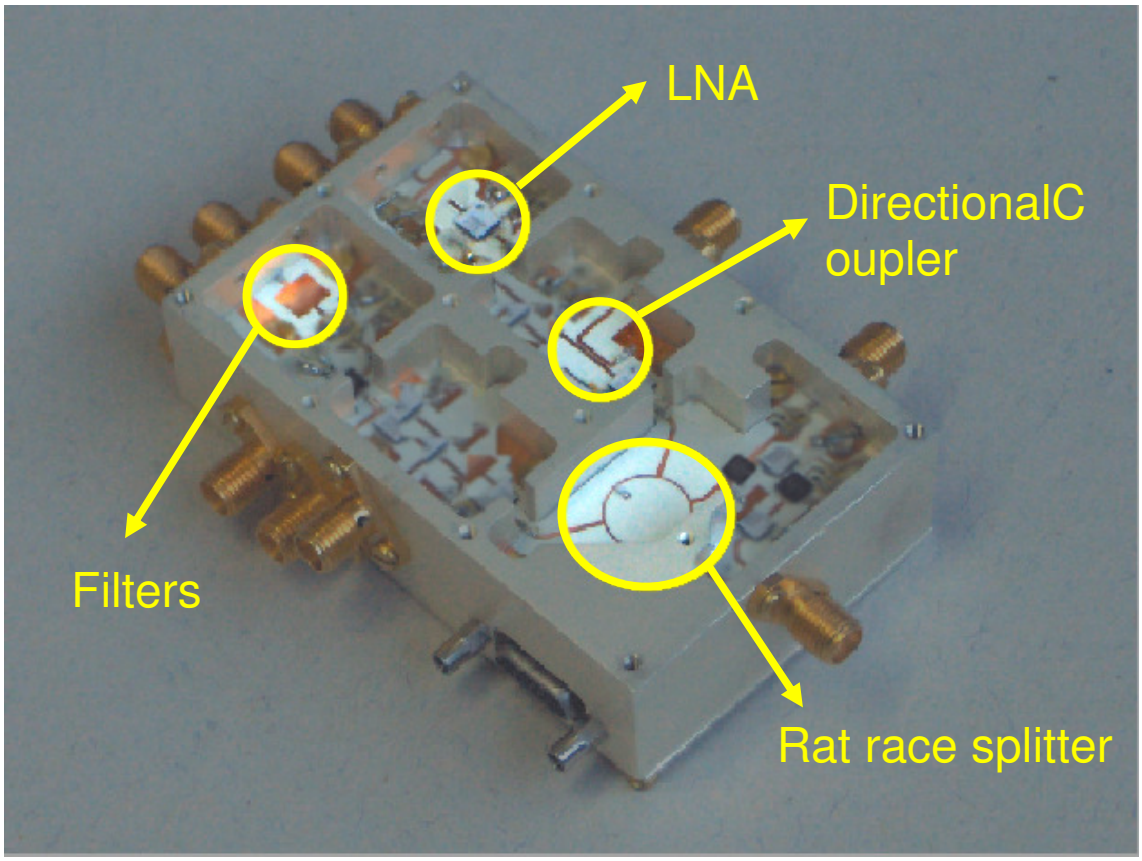

Fig. 4 A hybrid circuit realized by using a soft substrate and enclosed in a purposely designed case with input, output and test connectors.

Unlike the MIC, the Monolithic Microwave Integrated Circuits (MMIC) are the true integrated circuits for RF and microwave applications in that they are entirely realized by specialized silicon foundry on the same substrate (active, passive and interconnections). MMIC are realized on Silicon (Si), Gallium Arsenide (GaAs) or other suited substrates by using modern technologies for integrated circuits which allow the realization of entire cells, blocks and, some times, entire systems on the same chip. With respect to MIC, MMIC allow better performances in terms of maximum operating frequency, dimensions, reliability and power efficiency, but their utilization

can be considered just for large scale production. In fact, it must be taken into account the fact that an Integrated Circuit requires the preliminary realization of the masks and the availability of a suited technological process. The cost of the masks and the access to the technological facilities makes advantageous the utilization of MMIC technology just in case of a large scale production (hundreds of thousand of pieces or more). Moreover, it must be considered that the possibility of realize distributed elements on MMIC (transmission lines, matching networks, filters, power combiner and divider. etc.) is restricted to the higher frequency range of interest for Microwave. In fact, the dimensions of distributed devices are comparable with the wavelength so that their realization on a chip is made possible just above a few tens of GHz, that is for wavelength in the range of millimiters.

6.3.1 The substrates

Two types of substrates are normally used for MIC: soft and hard. Soft substrates make use of materials similar to Teflon (Diclad, Duroid etc.). The relative permittivity is between 2 and 3, they are light, quite flexible, cheaper than hard substrates. Soft substrates are mainly used in the frequency range between a few GHz and a few tens of GHz, up to the millimiter wave range. Above this limit, hard substrates have to be used because the dielectric losses in soft substrate increase together with parasitic and spurious effects which cause a performance degradation in terms of gain and power dissipation .

Hard substrates make use of high permittivity material, for instance Alumina (AL_2O_3) or Berillium Oxide. The relative permittivity is around 10 or more: this fact has a positive effect on the dimensions of distributed elements in that the wavelength is reduced by a factor 3 or more, with respect to air, therefore the dimensions of transmission lines, matching networks, filters and so on, are reduced by the same factor. By using hard substrates it is possible to realize MIC in the frequency range up to 100 GHz or more.

Both, soft and hard, substrates are constituted by a dielectric sheet with a double metallization, in the top and down surface. The down surface metallization is used as ground plane whereas, in the upper metallization layer, suited geometries can be realized by using standard photo-lithographic process. In this way different passive devices, such as power combiners and dividers, directional couplers, spiral inductors, planar transformer and balun, inter-digitated capacitors and so on, can be realized [12].

Furthermore, by using a little more complex technological processes than lithographic one, the deposition of thin metal film, ceramic pastes, and insulating layer is made possible, so allowing the

realization on the substrate of passive devices, such as resistors, metal-insulator-metal (MIM) capacitors and multilayer inductors and transformers. Finally, it must be pointed out that in planar MIC (regardless on the substrate type) different typologies of planar antennas (dipole, patch, slotted, etc. both active and passive) can be realized as well as high directivity antenna arrays with or without electron beam forming. In other words, with MIC technology an entire microwave transmitter-receiver system, included antennas, LNA and power amplifier can be designed, simulated and realized *in house* by using quite low cost instrumentation and facilities.

6.3.2 Design, simulation and realization of Microwave Integrated Circuits

Several CAD tools are available for the design and simulation of MIC, but the most complete and widespread one is ADS (Advanced Design System) by Agilent Technologies. ADS makes available a very complete integrated simulation tool starting from the bottom level of the Electromagnetical simulation of circuits, antennas and case, up to the top level of the entire communication system simulation.

Furthermore, a specific ADS module makes available the integration with Cadence, the most widespread CAD tool for integrated circuits design. In this way, the design kit of a particular technological process for integrated circuits production (for instance: 65 nm CMOS by STMicroelectronics) can be used in ADS environment for design and simulation, then the final circuit design can be transferred to the silicon foundry for large scale production. In other words, by using ADS, both MIC and MMIC can be designed and simulated. In Fig. 5 a typical screenshot of ADS is shown.

After the simulation, when the results comply with the initial specifications, the layout of the circuits is extracted and the board with passive distributed devices and the slots for passive and active discrete devices is realized.

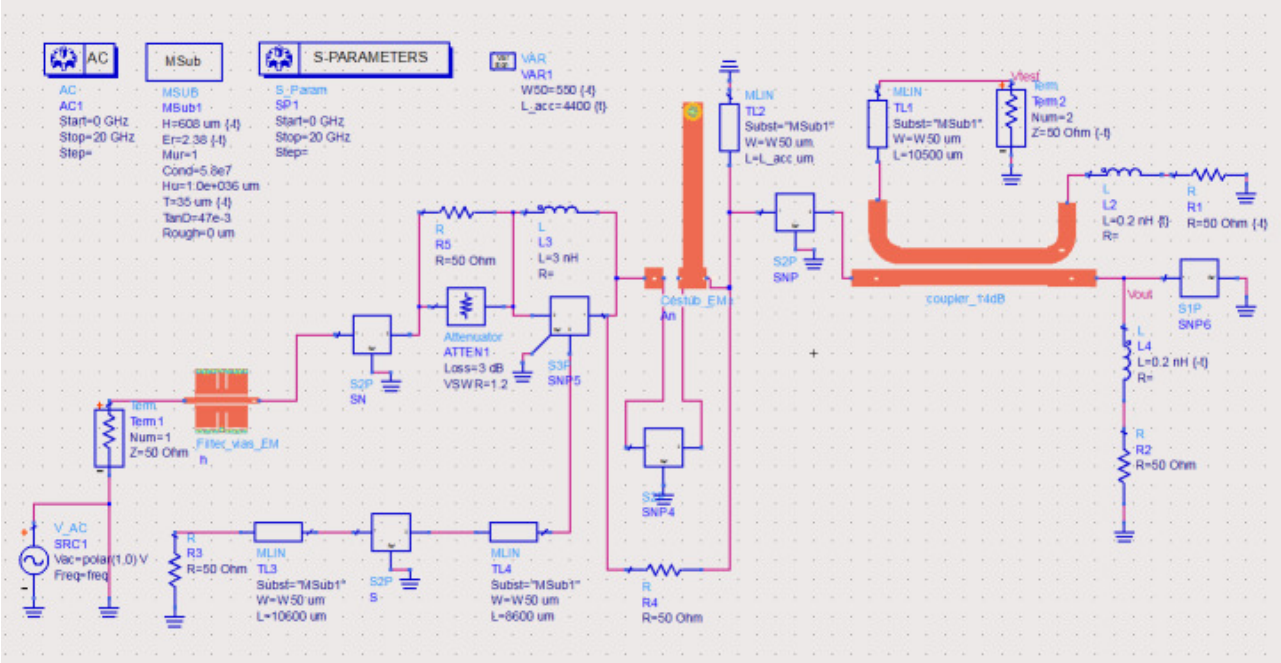

Fig. 5 ADS screenshot of the receiver section of a RADAR Doppler.

6.4 Low Cost RADAR Prototype for Harbour Surveillance

The target of this project was the design, simulation, realization and testing of a low power (a few watts), low cost (less than 1.000 $ for radio front end) RADAR, capable of monitoring the presence, and tracking the movements, of any kind of ship inside and in the neighboring of a harbour. The RADAR sensor should be able to make 3D imaging of ships and vessels with a resolution of about 0.5 m. To this end a single transmitting antenna and three receiving channels connected to three antennas in spatial diversity, in order to allow interferometric analysis, will be used. The way in which 3D reconstruction can be accomplished is beyond the scope of the present book, so that we will examine in the following the single channel RADAR front-end, that is the RADAR with only one receiving antenna. The overall design of the harbour surveillance system is based on a wireless sensor network whose node are single RADAR sensors distributed in the harbour area, allowing the data fusion at network level of the imaging coming from all of the nodes. The entire network could be constituted by some tens of RADAR sensors which should be characterized by low dissipated power, small dimensions and, first of all, a low level of EM pollution.

A FMCW solution is the most suited for such an application, which is capable of giving information both on the distance R and on the radial velocity V_R of the target, by using quite low values of the output power (a few watts) for some kilometers of coverage range.

The typical block diagram of a FMCW RADAR front-end is shown in Fig. 6.

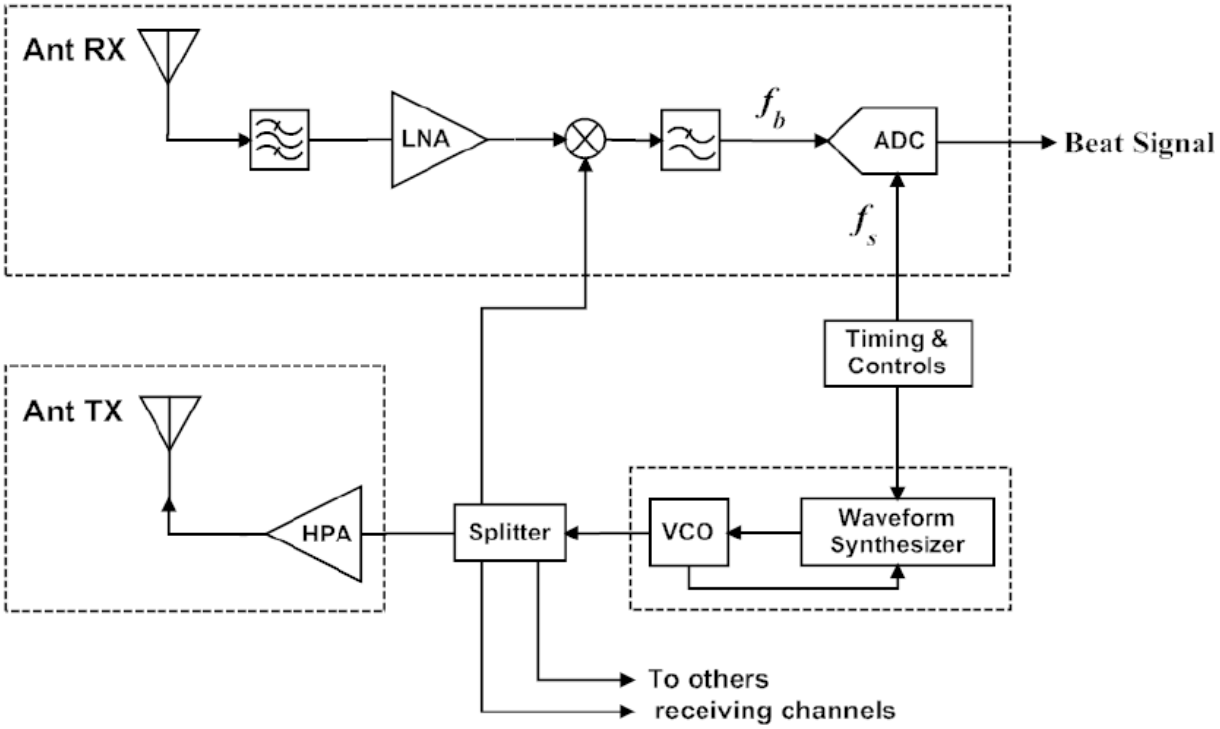

Fig. 6 Block diagram of a FMCW RADAR front-end

6.4.1 Feasibility study and dimensioning

The principle of operation of the HS RADAR can be summarized as follows. The instantaneous frequency transmitted by the output antenna is $f_T(t) = f_{MIN} + At$. Whether a target at a distance d reflects the transmitted wave, the back scattered wave arrives at the receiving antenna with a delay $\tau = 2d/c$. So that the received frequency at instant t is $f_R(t) = f_{MIN} + A(t - \tau)$ at the output of the mixer at time t we have a frequency f_{IF} equal to the difference between f_T *and* f_R that is:

$$f_{IF} = A\tau = A2d/c \qquad (6.3)$$

By measuring f_{IF} the value of d can be evaluated provided that A is known.

The specifications were:

- Frequency: X Band (8-12.5 GHz)
- Waveform: FMCW
- Antenna : 60° azimut
- Range: > 1.5 Km
- Range resolution: 0.5 m

- Receiver dynamics: > 96 dB
- SNR at the receiver output : SNR ≥ 20 dB
- Channel number : 3 (for 3D imaging)
- Maximum Output power: 10 W

The FM band depends on the required resolution through the well known relationship:

$$B = \frac{c}{2d_R} \qquad (6.4)$$

where $B = f_{MAX} - f_{MIN}$ is the difference between the maximum (f_{MAX}) and minimum (f_{MIN}) instantaneous value of the frequency, c is the light velocity in air and d_R is the distance (or range) resolution. Eq. 6.4 for the required resolution of 0.5 m gives a value of 300 MHz, therefore the values of f_{MIN} and f_{MAX} have been chosen equal to 10.5 and 10.8 GHz.

The behaviour of the instantaneous frequency of the transmitted constant wave is shown in Fig. 7 where T_{SW} is the rise time, that is the time required for the instantaneous frequency to rise from its minimum value f_{MIN} to its maximum value f_{MAX}. During a time interval T_{SW} the instantaneous frequency f rises up with a velocity A where A is measured in s^{-2}. The instantaneous frequency is generated by a VCO (Voltage Controlled Oscillator) inserted in a PLL (Phase Locked Loop) which can be digitally controlled by a microcontroller (μC). The μC send a trigger signal at the beginning of each new frequency ramp to the DSP in order to allow synchronization. It is worth to underline that the frequency reference of the PLL is a crystal oscillator which continuously oscillates at its resonance frequency, so that the phase coherence of the generated FMCW over different ramps is guaranteed by the synchronization with the same reference oscillation. The coherence accuracy depends only on the phase noise of the reference source. Maximum values of A for commercial PLL, for frequencies around 10 GHz, are in the range of 10^{12} s^{-2} [13]. For higher values of A, the VCO linearity is no longer guaranteed and the generated instantaneous frequency shows a more complicated dependence on time t: this has to be avoided for a correct and simple application of FMCW principle of operation.

As far as the SNR at the receiver output is concerned, it depends on the following quantities: the output power P_{CW} of the transmitter , the Noise figure N_F of the receiver, the cross radar section σ of the target, the transmitting and receiving antenna gain (G_{TX} and G_{RX} respectively), the total losses L in air and inside the system, the maximum distance R_P of the target, the equivalent available total

noise power spectral density $N_0=KTN_F$, at the input of the receiver (for T=290K) , the bandwidth B_F of the filter at the output of the mixer receiver ,

$$SNR = \frac{P_{RX}}{kTB_F N_F} = \frac{P_{CW}\lambda^2 G^2}{(4\pi)^3}\frac{1}{L}\frac{\sigma}{R_P^4}\frac{1}{kTB_F N_F} \qquad (6.5)$$

In Eq. 6.5 P_{RX} represents the received power, whereas G_{TX} and G_{RX} have been supposed both equal to G.

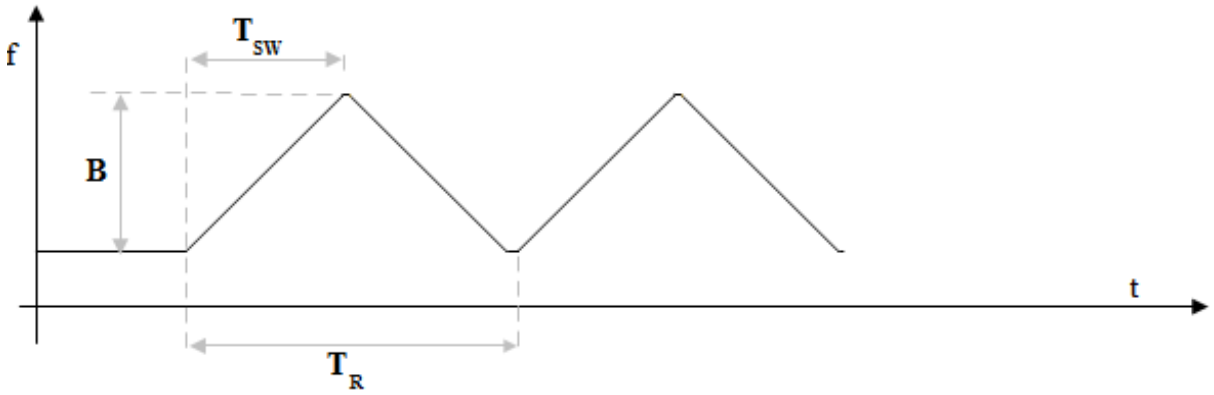

Fig. 7 Instantaneous frequency vs. time.

The output signal of the mixer, after amplification and filtering, is sampled and transferred to the digital domain for Digital Signal Processing (DSP). A Discrete Fourier Transform (DFT) is calculated on the sampled data, whose frequency resolution Δf is equal to the inverse of the time record length ΔT: $\Delta f = 1/\Delta T$. In digital domain the equivalent of the filter bandwidth B_F is the frequency resolution of the DFT, so that B_F has to be substituted by Δf in Eq. 6.5. In our case the time record length ΔT coincides with T_{SW} (see Fig. 7). Some details about the processing of the beat signal will be given in section 6.4.2.

As in the case of EH RADAR presented in section 6.2, also for the HS RADAR the SNR can be improved by a factor N, where N is the number of identical repetitions of the received signal, by integrating the output for a time $T_{INT} = N\,T_R = N/\Delta f$. That is $N = T_{INT}\,\Delta f$. The coherence, as already said, is guaranteed by the reference oscillator of the PLL.

The resulting value of the SNR after DSP with an integration time equal to T_{INT} , SNR_{OUT}, is given by

$$SNR_{OUT} = \frac{P_{CW}\lambda^2 G^2}{(4\pi)^3}\frac{1}{L}\frac{\sigma}{R_P^4}\frac{T_{INT}}{kTN_F} \qquad (6.6)$$

SNR_{OUT} is shown in Fig. 8 for different values of T_{int}. The value of the different parameters used for the evaluation are represented in the inset in the bottom of the figure, whereas the total loss L is the combined effect of air loss (L_{am}) and system loss (L_{sys}).

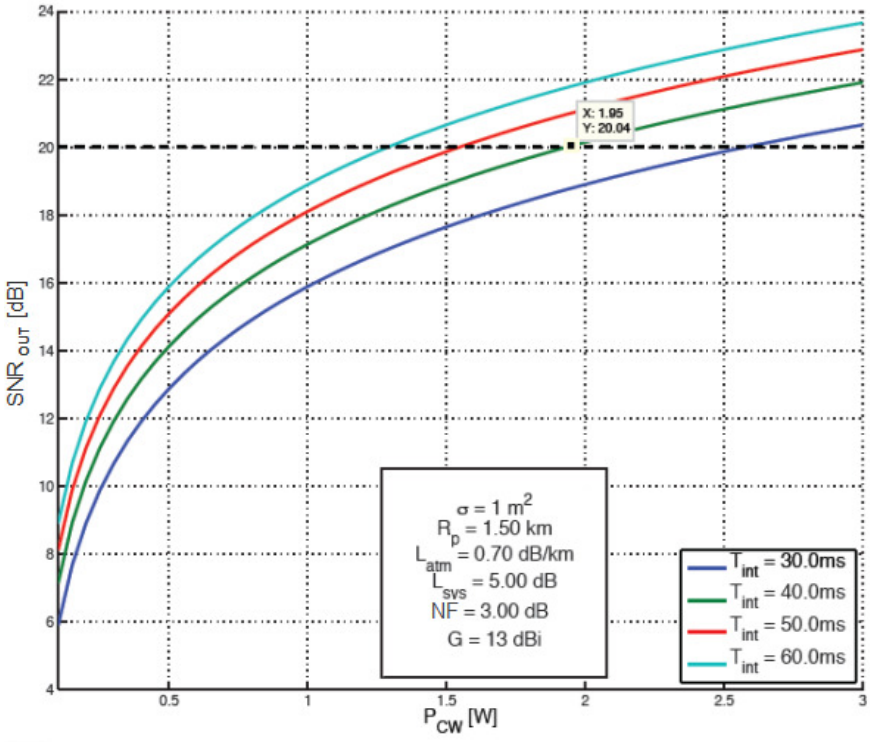

Fig. 8 Signal to Noise Ratio after DSP for different values of integration time T_{INT}.

A commercial horn antenna with 13 dBi gain has been used for the prototype testing, but a low cost patch antenna arrays (patent pending) realized by using a soft substrate will be used for the final version of HS RADAR (see paragraph 6.3 for a short description of the microwave hybrid circuit technology). Due to the low values of the target velocity (less than 50 Km/h), in a time interval of 40 ms the target displacement is less than 0.55 m, very similar to the required range resolution, therefore an integration time of 40 ms does not impair in a significant way the accuracy in the target movements reconstruction. This means (see Fig. 8) that a value of SNR_{OUT} of 20 dB can be obtained with an output power equal to 2W. Obviously, the positive effect of integration on SNR_{OUT} is effective just in the case in which the coherence can be guaranteed (see next section for this aspect).

Until now the effect of the relative velocity of the target with respect to the RADAR sensor, that is the Doppler effect, has been neglected. Due to this effect, in the case of a target moving toward the RADAR at a radial velocity v_R, the received frequency is shifted by a quantity Δf given by Eq. 6.1. It is worth noting that Δf is lower than 1 kHz for $v_R \leq 50 km/h$.

It is possible to show that, due to Doppler effect, in case of moving targets, the frequency f_{IF} (see Eq. 6.3) at the mixer output is shifted by - Δf in the half period in which the instantaneous frequency increases and by + Δf in the other half period. This means that the information on the velocity and on the distance of the target are both contained in the beat signal (see Fig.7) at the output of the RADAR front-end. An example of the way in which they can be extracted by means of DSP is presented in Chap. 5, Section 5.2.1 for automotive FMCW RADAR. For HS RADAR a different choice has been made: some details will be given in Section 6.4.3.

6.4.2 Realization

By taking into account the results of the feasibility study in section 6.4.1 and the availability of discrete and integrated devices on the market, the following specification have been carried out for the circuit blocks shown in Fig. 7.

Receiver NF (included ADC)	**≤ 5 dB**
LNA Gain	**29 dB**
Mixer conversion loss	**8 dB**
Minimum beat frequency (d=50m)	**200 KHz**
Maximum beat frequency(d=1250m)	**5 MHz**
IF band	**100 KHz – 5 MHz**
IF Gain	**43 dB**

A maximum output power of 2 W is obtained thank to the stage marked as HPA (High Power Amplifier) in Fig. 7. A hybrid PLL has been utilized with a VCO in the range of 10 - 12 GHz, capable of generating a FMCW with a maximum value of A in the required range of $10^{12} s^{-2}$ (a value

of $6x10^{11}s^{-2}$ has been chosen corresponding to T_{SW}=500 μs in order to obtained the required value of B=300 MHz).

The frequency range of the beat signal depends on the maximum distance which has to be covered. For the harbour surveillance, by considering also the fact that the complete coverage is obtained by installing a wireless RADAR sensor network, a suited coverage range for each sensor is 1.5 km. For d=1.5 km Eq. 6.3 gives f_{IF}= 6 MHz. A 6th order low pass Chebicev filter, with 6 MHz bandwidth, has been used as antialiasing filter before sampling the beat signal at a sampling rate of 12.5 MSa/s. The prototype of the system has been realized by using the hybrid technology described in Section 6.3. With reference to Fig. 6 the dotted lines circumscribe the part of the system contained in a single board; each board has been mounted in a custom designed case with microwave connectors in order to allow individual test before to proceed to a more compact single board realization of the prototype.

Several simulations have been carried out both at the circuit and system level by using ADS (see section 6.3); an example regarding the results of the simulation of the receiver stage (LNA + input filter) is presented in Fig. 9, where the parameters S21 (insertion gain) and S11(return loss) are shown.

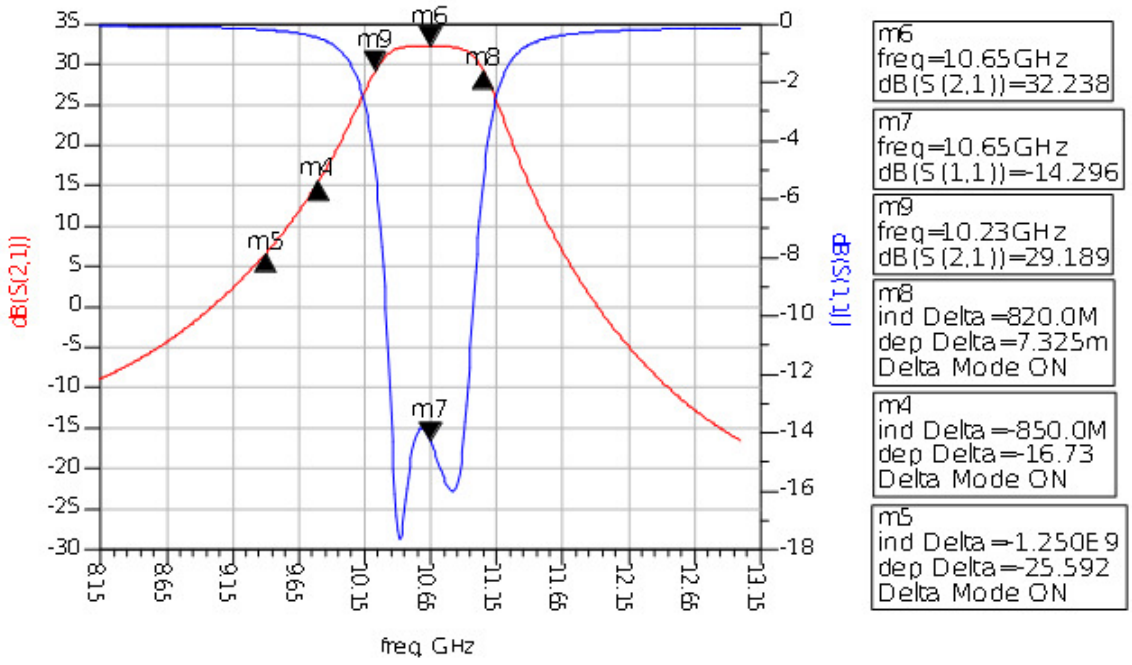

Fig. 9 Insertion gain (S21) and return loss (S11) of the receiver section of the HS RADAR front-end

In Fig. 10 the receiver section board is shown. Receiver and transmitter sections have been realized in separated boards to make easier the prototype test: they will be contained in the same compact shielded case in the final realization. The case will be connected to the antennas (receiving and transmitting) and to the power supply, whereas the low frequency output of the mixer, after low pass filtering and amplification (Test Port in Fig. 11) , will be made available for sampling and DSP.

For a single sample of the RADAR front end shown in Fig. 10, the cost of the devices, both active, passive, discrete and integrated and that for the realization of the board and of the case can be estimated around $ 500 (€ 370). It is evident that in the case of series production of several hundreds or thousands of sample the unitary cost would drop in a significant way (at least 50%).

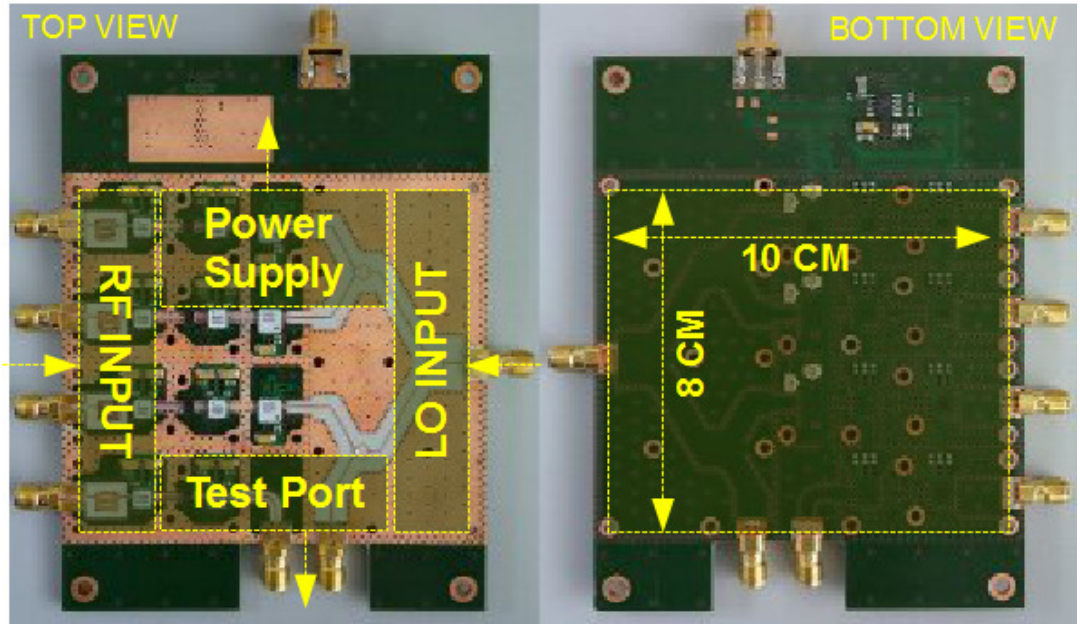

Fig. 10 The prototype of the receiver of the HS RADAR

6.4.3 Data processing

In this Section, some information will be given about the processing of the signal at the output of the RADAR front-end receiver.

After AD conversion at 12.5 MS/s with 14 bit resolution, the signal is ready for Digital Signal Processing. For SH RADAR prototype testing, DSP has been implemented in a Matlab platform running on a PC. In the final version of the RADAR, DSP will be performed on a dedicated board,

but the processing steps will be unchanged and the final result will be the identification of targets, inside the operating range of the RADAR, in terms of distance and radial velocity.

The processing algorithm is different from that described in Chapter 5, Section 5.2.1 for automotive FMCW RADAR. In fact, in order to detect radial velocities as low as 1 kn (1 nautical mile per hour), according with Eq. 6.1, the frequency resolution of FFT should be less than 36 Hz and, consequently, the time record length should be greater than 27.7 ms. This means that the number of samples for the FFT, at 12.5 MHz of sampling rate, should be greater than 347,222, that is 524,288 which is the closest power of 2. This would require the utilization of purposely designed and very expensive DSP for real time elaboration. For this reason, the processing algorithm, which has been implemented, is different: it consists of a two dimensional (2D) FFT, shortly described in the following.

First of all, the Coherent Period of Integration *CPI* has to be determined. *CPI* corresponds to the T_{INT} in Eq. 6.6. The serial flux of samples in a *CPI*, taken at a sampling period equal to 80 ns (the inverse of the sampling rate), is organized in a matrix with L rows and N columns. Each column contains the samples corresponding to a single, up or down, frequency ramp whose duration is T_{SW}. (see Fig. 7). The number of columns N is equal to CPI/T_{SW}, whereas the number of rows L is equal to the number of samples in $T_{SW.}$ For instance by using T_{SW} = 500 μs and CPI = 50 ms, it results N=100 and L=6250. In this way, two adjacent positions in the same column corresponds to consecutive samples of the beat signal (that is two samples taken at 80 ns each other), whereas two adjacent positions in the same row corresponds to samples of the beat signal taken at T_{SW} seconds each other. At this point, after suited correction, to take into account the fact that the range component of the beat frequency reverses sign when the direction of sweep is reversed, windowing and zero padding, a 2D FFT is performed on the matrix. A complete discussion about this topic is beyond the aim of this book and can be found, for instance, in [14]. Here, it is worth just to say that the result of 2D FFT, after proper elaboration, can be organized in a 3D map in which the radial velocity and the distance of a given target are represented in the *X* and *Y* axes respectively, and the "intensity" of the corresponding echo is represented in *Z* axis (or in a 2D graph, by using a false colour map).

The laboratory preliminary tests, hardware and data processing, showed that the performances of the HS RADAR match the required characteristics for radio front-end, but to verify the true resolution and sensitivity of the whole RADAR sensor network, a campaign of on field measurements has to be carried out in the future.

ACKNOWLEDGEMENT

The author wishes to thank Dr. R. Massini who designad, realized and tested the complete prototype of HS RADAR front-end and Dr. S. Lischi (Ph.D. University of Pisa) who implemented DSP algorithms.

REFERENCES

[1] L. Fanucci, S. Saponara, T. Bacchillone, M. Donati, P. Barba, I. Sanchez, C. Carmona, "Sensing devices and sensor signal processing for remote monitoring of vital signs in CHF patients" IEEE Transactions on Instrumentation and Measurements 2013

[2] E.M. Staderini, " UWB RADAR in Medicine", IEEE Aerospace and Electronic System Magazine, vol.17, pp. 13-18, Jan. 2002.

[3] J.C. Lin, "Microwave sensing and physiological movement and volume change: a review", Bioelectromagnetics, vol.13, pp.557-565, 1992.

[4] T.E. McEwan, "Body monitoring and imaging apparatus method", U.S.Patent 5 573 012, Nov. 12, 1996.

[5] I. J. Immoreev and S. V. Samkov, "Ultra-wideband RADAR for remote measuring of main parameters of patient's vital activity", Radio Physic and Radio Astronomy, vol.7, pp.404-407, 2002.

[6] D. Zito, D.Pepe, B.Neri, D. De Rossi, "Feasibility study of a low-cost System-on-a-chip UWB Pulse RADAR on Silicon for Heart Monitoring"; IEEE Waveform Diversity and Design Conference (WDD) 2007, pp. 32-36

[7] D. Zito, et al. "SoC CMOS UWB Pulse RADAR Sensor for contactless Respiratory Rate Monitoring" , IEEE Trans. Biomedical System and Circuits, Vol. 5, 2011.

[8] B. Neri, S. Saponara, "Advances in Technologies, Architectures and Applications of Highly-Integrated Low-power Radars, IEEE AEROSPACE AND ELECTRONIC SYSTEMS MAGAZINE, vol. 27/1, pp 25,tot.pag 12,2012

[9] C. Gabriel and S. Gabriel, "Compilation of the dielectric properties of body tissues at rf and microwave frequencies", 2000. Online: http://www.brooks.af.mil/AFRL/HED/hedr/reports/dielectric/home.html

[10] D. Zito, D. Pepe, M. Mincica, F. Zito, D. De Rossi, A. Lanata, E. P. Scilingo, A. Tognetti, "Wearable System-on-a-Chip UWB Radar for Contact-less Cardiopulmonary Monitoring: Present Status", 30th Annual International IEEE EMBS Conference, Vancouver, August 20-24, 2008, pp 5274-5277.

[11] D. Pepe, D. Zito, “Planar differential antenna for UWB pulse radar sensor”, COMCAS 2013, pp 1–4, IEEE CONFERENCE PUBLICATIONS

[12] D. M. Pozar, "Microwave engineering", 4th edition, Wiley, 2013

[13] See, as an example, IC PLL HMC70xxxxx series by Hittite at www.hittite.com.

[14] Mohinder Jankiraman, “Design of multi-frequency CW radars”, SciTech Pub., 2007.